

# SESAMI Web: An Accessible Interface for Surface Area Prediction from Adsorption Isotherms

Gianmarco G. Terrones<sup>1</sup>, Yu Chen<sup>2</sup>, Li-Chiang Lin<sup>3</sup>, Heather J. Kulik<sup>1,4</sup>, and Yongchul G. Chung<sup>2</sup>✉

<sup>1</sup> Department of Chemical Engineering, Massachusetts Institute of Technology, USA <sup>2</sup> School of Chemical Engineering, Pusan National University, South Korea <sup>3</sup> William G. Lowrie Department of Chemical and Biomolecular Engineering, The Ohio State University, USA <sup>4</sup> Department of Chemistry, Massachusetts Institute of Technology, USA ✉ Corresponding author

DOI: [10.xxxxxx/draft](https://doi.org/10.xxxxxx/draft)

## Software

- [Review](#) ↗
- [Repository](#) ↗
- [Archive](#) ↗

Editor: [Open Journals](#) ↗

Reviewers:

- [@openjournals](#)

Submitted: 01 January 1970

Published: unpublished

## License

Authors of papers retain copyright and release the work under a Creative Commons Attribution 4.0 International License (CC BY 4.0).

## Statement of need

Surface area determination is important for the evaluation of a porous material's viability in applications ranging from catalysis to separations to gas storage. The most widely used approach for the evaluation of a material's specific surface area, i.e. surface area per unit mass, is Brunauer-Emmett-Teller (BET) theory (Brunauer et al., 1938). Given the adsorption isotherm of a gas in an adsorbent, one can use BET theory to determine the specific surface area of the adsorbent upon identification of an appropriate linear region in the isotherm. This procedure is sometimes automatically performed by the software program that comes with the commercial adsorption apparatus that measures the adsorption isotherm. Unfortunately, the linear region selection is a large source of variability in BET-calculated areas. In addition, for certain types of isotherms, automatic selection of the linear region by the commercial software sometimes fails. As a result, many researchers perform the analyses manually on a spreadsheet, which can become time-consuming and nearly impossible for some types of isotherms (Osterrieth et al., 2022). These challenges have motivated the development of programs for the automated determination of BET areas (Datar et al., 2020; Iacomi & Llewellyn, 2019; Osterrieth et al., 2022; Sadeghi et al., 2020; Sinha et al., 2019). Furthermore, shortcomings of BET as a tool for surface area calculation, such as its relatively poor performance in treating high surface area materials with multimodal pore sizes (Gómez-Gualdrón et al., 2016; Wang et al., 2015), have led to the development of alternate methods for surface area calculation from isotherms (Datar et al., 2020; Sinha et al., 2019).

## Summary

In contrast to previously developed programs which require use of the command line (Iacomi & Llewellyn, 2019; Osterrieth et al., 2022) and familiarity with Python (Datar et al., 2020; Iacomi & Llewellyn, 2019; Sinha et al., 2019), the SESAMI web interface allows a user to generate surface area predictions on their web browser by uploading isotherm data. The website facilitates access to the previously developed SESAMI models (SESAMI 1 and 2) for porous material surface area prediction (Datar et al., 2020; Sinha et al., 2019) and has been tested by experimental groups. The motivation for this interface is to lower the barrier of entry for research groups seeking to use SESAMI code, which was previously packaged in Python and Jupyter Notebook scripts.

SESAMI 1 applies computational routines to identify suitable linear regions of adsorption isotherms for Brunauer-Emmett-Teller surface area prediction (Fagerlund, 1973). The automated workflow includes consideration of Rouquerol criteria (J. Rouquerol et al., 2007; Jean

42 [Rouquerol et al., 2013](#)) and the use of coefficients of determination as a measure of linearity.  
 43 Furthermore, SESAMI 1 supports a combined BET+ESW (excess sorption work) approach  
 44 for linear region selection; this combined approach has been shown to outperform the BET  
 45 approach in some cases ([Sinha et al., 2019](#)). A user can specify a cutoff  $R^2$  and a minimum  
 46  $R^2$ , such that a candidate linear region is favored to be selected if it has an  $R^2$  above the  
 47 cutoff, and a candidate linear region is only considered if it has an  $R^2$  above the minimum. On  
 48 the other hand, SESAMI 2 applies a machine learning (specifically, regularized linear regression  
 49 with LASSO) model for the accurate surface area prediction of high surface area materials,  
 50 improving on BET performance for these materials ([Datar et al., 2020](#)). The LASSO model  
 51 uses as input the average loading in seven isotherm pressure regions as well as pairwise products  
 52 of these loadings. The SESAMI routines support isotherms with  $N_2$  and argon adsorbate at 77  
 53 K or 87 K, respectively.

54 The SESAMI web interface has extensive error handling and clearly alerts users of issues with  
 55 their adsorption isotherm data. For example, it alerts the user if no ESW minima is found  
 56 by SESAMI 1 or if the data is incompatible with SESAMI 2 code due to data sparsity in  
 57 certain pressure regions. As shown in [Figure 1](#), the interface displays SESAMI 1 calculation  
 58 results including information on the chosen linear region, namely the satisfied Rouquerol criteria  
 59 ([J. Rouquerol et al., 2007](#); [Jean Rouquerol et al., 2013](#)), the pressure range and number of  
 60 data points in the region, and the coefficient of determination. The interface also displays  
 61 intermediate SESAMI 1 values for surface area calculation, namely the BET constant,  $C$ , and  
 62 the monolayer adsorption loading,  $q_m$ . Furthermore, the SESAMI web interface allows the user  
 63 to download figures generated by SESAMI 1 that indicate, among other things, the chosen  
 64 linear monolayer loading regions by the BET and BET+ESW approaches as well as the excess  
 65 sorption work plot ([Figure 1](#)). The user can convert output from commercial equipment to  
 66 AIF format and upload the converted data to the interface for analysis. The SESAMI web  
 67 interface is publicly available at <https://sesami-web.org/>, and source code is available at  
 68 [https://github.com/hjkgrp/SESAMI\\_web](https://github.com/hjkgrp/SESAMI_web).

<b>a)</b>	<p><b>SESAMI 1.0 (BET) results are:</b></p> <p>BET area = 2430.9 m<sup>2</sup>/g  C = 201.1  q<sub>m</sub> = 28.42 mol/kg  Rouquerol consistency criteria 1 and 2: Yes  Rouquerol consistency criterion 3: Yes  Rouquerol consistency criterion 4: Yes  Number of points in linear region: 9  Lowest pressure of linear region: 3500 Pa  Highest pressure of linear region: 8000 Pa  R<sup>2</sup> of linear region: 0.9996</p>	<p><b>SESAMI 1.0 (BET+ESW) results are:</b></p> <p>BET area = 2346.7 m<sup>2</sup>/g  C = 248.1  q<sub>m</sub> = 27.44 mol/kg  Rouquerol consistency criteria 1 and 2: Yes  Rouquerol consistency criterion 3: No  Rouquerol consistency criterion 4: Yes  Number of points in linear region: 9  Lowest pressure of linear region: 600 Pa  Highest pressure of linear region: 1500 Pa  R<sup>2</sup> of linear region: 0.9985</p>
	<p><b>SESAMI 2.0 (LASSO) surface area prediction is:</b></p> <p>2099.1 m<sup>2</sup>/g</p>	

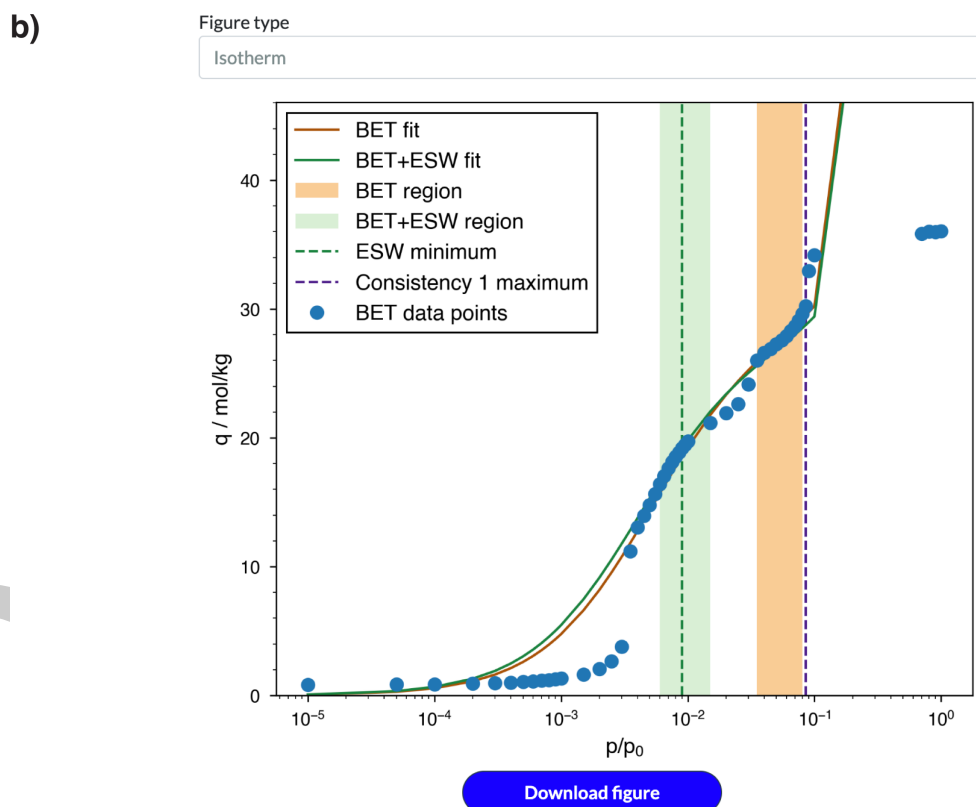


**Figure 1:** Information displayed by the SESAMI web interface after a calculation has been run. a) Interface printout of information on the SESAMI 1 chosen linear regions, and SESAMI 1 and 2 calculation results. b) Figure download functionality for figures detailing SESAMI 1 calculation.

## 69 Benchmarking

70 To assess the performance of SESAMI code in predicting surface areas from isotherms, we  
71 benchmarked the SESAMI routines against other similar programs for 13 simulated and 9  
72 experimental N<sub>2</sub> isotherms obtained at 77 K for 14 metal-organic frameworks, some of which  
73 are shown in Figure 2. Simulated isotherms were obtained from Grand Canonical Monte  
74 Carlo (GCMC) simulations using RASPA open-source software (Dubbeldam et al., 2016),  
75 and experimental adsorption isotherms were obtained from the experimental data reported

76 by Islamoglu and coworkers (Islamoglu et al., 2022). The data were then used to calculate  
77 the surface areas from the SESAMI website, BETSI (Osterieth et al., 2022; Rampersad et  
78 al., 2020), pyGAPS (Iacomini, 2019; Iacomini & Llewellyn, 2019), and BEaTmap (Sadeghi et al.,  
79 2020).

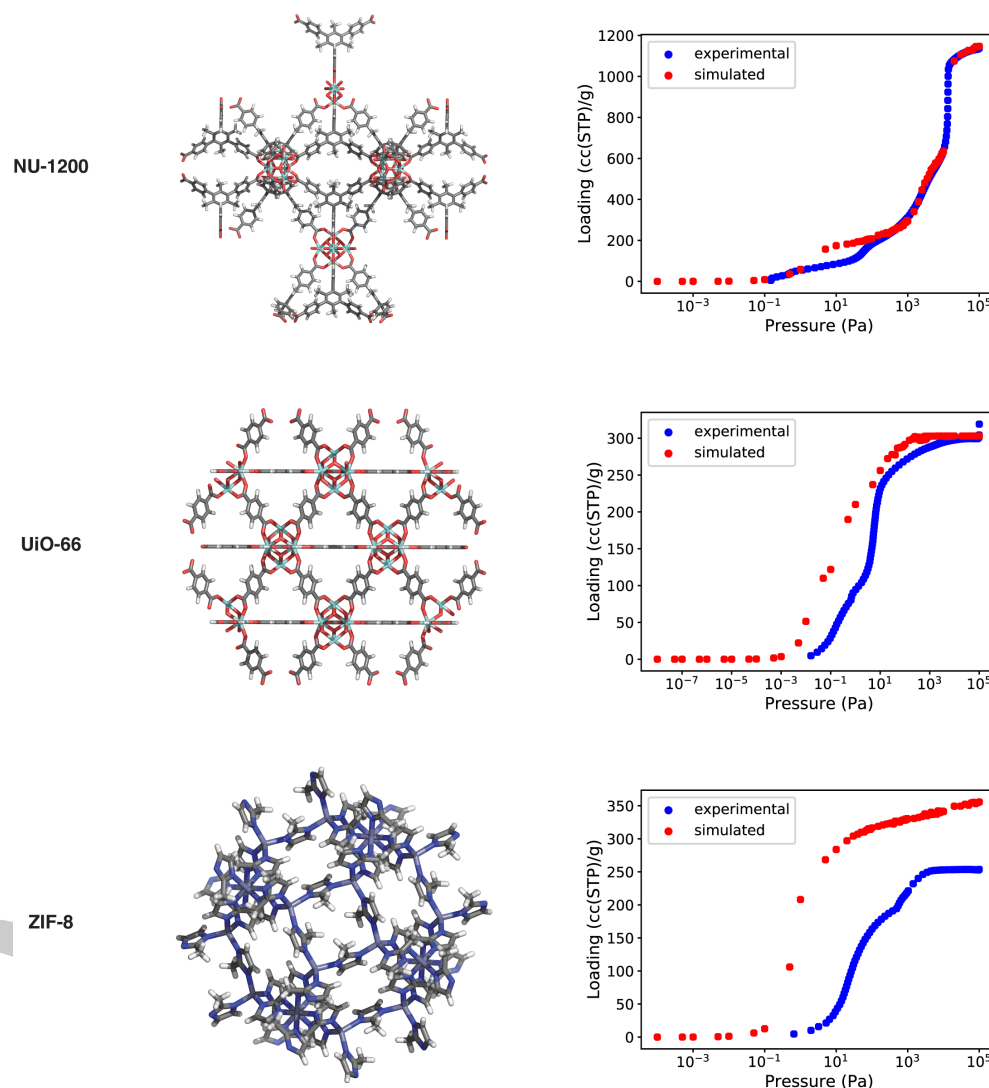


**Figure 2:** The crystal structures and isotherms of 3 of the 14 metal-organic frameworks used to benchmark different isotherm to surface area codes.

80 We find that over the set of 13 GCMC isotherms, the SESAMI machine learning model  
81 and BEaTmap have the best correlation with Zeo++ surface areas (Willems et al., 2012)  
82 calculated with a 1.67 Å probe N<sub>2</sub> molecule (Tables 2 and 1). Nevertheless, all software  
83 are in generally good agreement, underscoring the benefit of a computational approach to  
84 surface area calculation. The agreement between software is also not surprising due to the  
85 similar approach taken by most of the codes of considering multiple subsets of consecutive  
86 data points and applying checks like the Rouquerol criteria to select a linear region for BET  
87 analysis. Indeed, this agreement is also observed over the 9 experimental isotherms (Table 3).  
88 The benchmark isotherms, XLSX files of surface area predictions across different software tools  
89 for both GCMC and experimental isotherms, details about settings used for each software,  
90 and employed analysis scripts are available at [https://github.com/hjkgrp/SESAMI\\_web](https://github.com/hjkgrp/SESAMI_web).

**Table 1:** Calculated surface areas ( $\text{m}^2/\text{g}$ ) for the 13 MOFs with GCMC isotherms. Cases where a software does not find a surface area are denoted by N/A. Zeo++ calculations were conducted with the same CIF files used to generate GCMC isotherms, and a 1.67 Å probe  $\text{N}_2$  molecule, the high accuracy flag, and 2,000 samples were used. All other software took as input the GCMC isotherms.

	SESAMI 1 (BET)	SESAMI 1 (BET+ESW)	SESAMI 2 (LASSO)	BETSI	py- GAPS	BEaTmap	Zeo++
HKUST-1	2001	1933	2089	1962	1902	1980	2397
IRMOF-1	3502	3543	3123	3519	3504	N/A	3722
MIL-100 (Cr)	2107	1853	2111	N/A	1852	2094	1957
MIL-100 (Fe)	2386	2438	2203	2426	82	2423	1933
MIL-101	3828	2862	2944	N/A	2939	3331	3164
MIL-53 (Al)	1221	1168	1405	1164	1183	1212	1510
MOF-74 (Mg)	1828	1834	1902	N/A	1839	1791	1796
MOF-808	44	N/A	1275	N/A	N/A	1147	1690
NU-1000	2439	2181	2633	N/A	2144	2672	3050
NU-1200	2711	934	2601	N/A	1073	2930	3192
NU-1500 (Fe)	3543	3594	3111	N/A	3758	3492	3944
UiO-66	1239	1239	1443	N/A	1242	1304	1289
ZIF-8	1429	1386	1575	1381	1390	1414	1588

**Table 2:** Comparison between surface area predictions from Zeo++ and software for isotherm to surface area calculation, over the 13 MOFs with GCMC isotherms. The number of successful isotherm to surface area calculations for each software are indicated as well.

Surface area calculation software	Mean Absolute Percent Error (MAPE)	Pearson correlation coefficient	Successful calculations
SESAMI 1 (BET)	19.4	0.85	13
SESAMI 1 (BET+ESW)	17.9	0.72	12
SESAMI 2 (LASSO)	12.4	0.95	13
BETSI	17.0	0.92	5
pyGAPS	23.0	0.75	12
BEaTmap	12.6	0.93	12

**Table 3:** Calculated surface areas ( $\text{m}^2/\text{g}$ ) for the 9 MOFs with experimental isotherms. Cases where a software does not find a surface area are denoted by N/A. All other software took as input the experimental isotherms.

	SESAMI 1 (BET)	SESAMI 1 (BET+ESW)	SESAMI 2 (LASSO)	BETSI	py- GAPS	BEaTmap
HKUST-1	1505	1466	1668	N/A	1495	1498
MOF-74 (Mg)	1580	1467	1692	N/A	1574	1565
MOF-808	1998	900	1727	N/A	2439	1752
NU-1000	2154	2090	2385	N/A	2654	2459
NU-1200	2893	2718	2781	2758	3917	3069

	SESAMI 1 (BET)	SESAMI 1 (BET+ESW)	SESAMI 2 (LASSO)	BETSI	py- GAPS	BEaTmap
NU-1500 (Fe)	3305	3409	2809	N/A	3413	3227
SIFSIX-3 (Ni)	356	201	716	N/A	355	353
UiO-66	1251	1228	1413	1250	1249	1246
ZIF-8	1092	910	1214	N/A	1082	1047

## Acknowledgements

This publication was made possible by the generous support of the Government of Portugal through the Portuguese Foundation for International Cooperation in Science, Technology and Higher Education and was undertaken in the MIT Portugal Program. Software and website development was supported by the Office of Naval Research under grant number N00014-20-1-2150, as well as by the National Research Foundation of Korea (NRF) under grant number 2020R1C1C1010373 funded by the government of Korea (MSIT). We thank Omar Farha, Timur Islamoglu, and Karam Idrees for kindly providing the raw data of the experimental isotherms in the work by Islamoglu et al. (2022).

## References

- Brunauer, S., Emmett, P. H., & Teller, E. (1938). Adsorption of Gases in Multimolecular Layers. *Journal of the American Chemical Society*, 60(2), 309–319. <https://doi.org/10.1021/ja01269a023>
- Datar, A., Chung, Y. G., & Lin, L. (2020). Beyond the BET Analysis: The Surface Area Prediction of Nanoporous Materials Using a Machine Learning Method. *The Journal of Physical Chemistry Letters*, 11. <https://doi.org/10.1021/acs.jpclett.0c01518>
- Dubbeldam, D., Calero, S., Ellis, D. E., & Snurr, R. Q. (2016). RASPA: Molecular Simulation Software for Adsorption and Diffusion in Flexible Nanoporous Materials. *Molecular Simulation*, 42(2), 81–101. <https://doi.org/10.1080/08927022.2015.1010082>
- Fagerlund, G. (1973). Determination of Specific Surface by the BET Method. *Matériaux Et Construction*, 6, 239–245. <https://doi.org/10.1007/BF02479039>
- Gómez-Gualdrón, D. A., Moghadam, P. Z., Hupp, J. T., Farha, O. K., & Snurr, R. Q. (2016). Application of Consistency Criteria to Calculate BET Areas of Micro- and Mesoporous Metal–Organic Frameworks. *Journal of the American Chemical Society*, 138(1), 215–224. <https://doi.org/10.1021/jacs.5b10266>
- Iacomì, P. (2019). *pyGAPS 4.4.0 documentation*. Sphinx. <https://pygaps.readthedocs.io/en/master/>
- Iacomì, P., & Llewellyn, P. L. (2019). pyGAPS: a Python-Based Framework for Adsorption Isotherm Processing and Material Characterisation. *Adsorption*, 25. <https://doi.org/10.1007/s10450-019-00168-5>
- Islamoglu, T., Idrees, K. B., Son, F. A., Chen, Z., Lee, S.-J., Li, P., & Farha, O. K. (2022). Are You Using the Right Probe Molecules for Assessing the Textural Properties of Metal–Organic Frameworks? *Journal of Materials Chemistry A*, 10(1), 157–173. <https://doi.org/10.1039/D1TA08021K>
- Osterrieth, J. W. M., Rampersad, J., Madden, D., Rampal, N., Skoric, L., Connolly, B., Allendorf, M. D., Stavila, V., Snider, J. L., Ameloot, R., & others. (2022). How

- 127        Reproducible are Surface Areas Calculated from the BET Equation? *Advanced Materials*,  
128        34. <https://doi.org/10.1002/adma.202201502>
- 129        Rampersad, J., Osterrieth, J. W., & Rampal, N. (2020). *Betsi-gui*. GitHub. <https://github.com/nakulrampal/betsi-gui>
- 130
- 131        Rouquerol, J., Llewellyn, P., Rouquerol, F., & others. (2007). Is the BET Equation Applicable  
132        to Microporous Adsorbents? *Stud. Surf. Sci. Catal*, 160(07), 49–56.
- 133        Rouquerol, Jean, Rouquerol, F., Llewellyn, P., Maurin, G., & Sing, K. S. (2013). *Adsorption*  
134        *by Powders and Porous Solids: Principles, Methodology and Applications*. Academic press.  
135        <https://doi.org/10.1016/B978-0-12-598920-6.X5000-3>
- 136        Sadeghi, A., Bell, E., & Gostick, J. (2020). *Beatmap v0.1.2*. GitHub. [https://github.com/](https://github.com/PMEAL/beatmap)  
137        [PMEAL/beatmap](https://github.com/PMEAL/beatmap)
- 138        Sinha, P., Datar, A., Jeong, C., Deng, X., Chung, Y. G., & Lin, L. (2019). Surface Area  
139        Determination of Porous Materials Using the Brunauer–Emmett–Teller (BET) Method:  
140        Limitations and Improvements. *The Journal of Physical Chemistry C*, 123. <https://doi.org/10.1021/acs.jpcc.9b02116>
- 141
- 142        Wang, T. C., Bury, W., Gómez-Gualdrón, D. A., Vermeulen, N. A., Mondloch, J. E., Deria, P.,  
143        Zhang, K., Moghadam, P. Z., Sarjeant, A. A., Snurr, R. Q., & others. (2015). Ultrahigh  
144        Surface Area Zirconium MOFs and Insights into the Applicability of the BET Theory.  
145        *Journal of the American Chemical Society*, 137(10), 3585–3591. [https://doi.org/10.1021/](https://doi.org/10.1021/ja512973b)  
146        [ja512973b](https://doi.org/10.1021/ja512973b)
- 147        Willems, T. F., Rycroft, C. H., Kazi, M., Meza, J. C., & Haranczyk, M. (2012). Algorithms  
148        and Tools for High-Throughput Geometry-Based Analysis of Crystalline Porous Materials.  
149        *Microporous and Mesoporous Materials*, 149(1), 134–141. [https://doi.org/10.1016/j.](https://doi.org/10.1016/j.micromeso.2011.08.020)  
150        [micromeso.2011.08.020](https://doi.org/10.1016/j.micromeso.2011.08.020)